Mol. Cells *32*, 589-595, December 31, 2011
DOI/10.1007/s10059-011-0197-1

Molecules and Cells

Structural Insights into the Conformational Diversity of ClpP from *Bacillus subtilis*

Byung-Gil Lee, Min Kyung Kim, and Hyun Kyu Song*

ClpP is a cylindrical protease that is tightly regulated by Clp-ATPases. The activation mechanism of ClpP using acyldepsipeptide antibiotics as mimics of natural activators showed enlargement of the axial entrance pore for easier processing of incoming substrates. However, the elimination of degradation products from inside the ClpP chamber remains unclear since there is no exit pore for releasing these products in all determined ClpP structures. Here we report a new crystal structure of ClpP from *Bacillus subtilis*, which shows a significantly compressed shape along the axial direction. A portion of the handle regions comprising the heptameric ring-ring contacts shows structural transition from an ordered to a disordered state, which triggers the large conformational change from an extended to an overall compressed structure. Along with this structural change, 14 side pores are generated for product release and the catalytic triad adopts an inactive orientation. We have also determined *B. subtilis* ClpP inhibited by diisopropylfluoro-phosphate and analyzed the active site in detail. Structural information pertaining to several different conformational steps such as those related to extended, ADEP-activated, DFP-inhibited and compressed forms of ClpP from *B. subtilis* is available. Structural comparisons suggest that functionally important regions in the ClpP-family such as N-terminal segments for the axial pore, catalytic triads, and handle domains for the product releasing pore exhibit intrinsically dynamic and unique structural features. This study provides valuable insights for understanding the enigmatic cylindrical degradation machinery of ClpP as well as other related proteases such as HslV and the 20S proteasome.

INTRODUCTION

The Clp-family comprises members involved in energy-dependent protease systems that play important roles in protein quality control by removing misfolded or damaged proteins as well as no longer needed short-lived regulatory proteins to avoid potential aggregation (Baker and Sauer, 2006; Gottesman, 2003). Clp proteases contain two distinct functional components, Clp-ATPase which acts as an unfoldase/chaperone, and ClpP which acts as a peptidase. Clp-ATPases such as ClpX and ClpA (ClpC and ClpE in the case of *Bacillus subtilis*) are hexameric AAA+ ATPases (ATPases associated with a variety of cellular activities) which recognize, unfold and translocate substrates to the protease component. ClpP is a serine protease consisting of two stacked heptameric rings with a small central entrance pore, and forms a complex with Clp-ATPases named ClpAP or ClpXP. Under physiological conditions, ClpP has only limited activity to degrade small peptides on its own, and mostly functions as a complex with Clp-ATPases (Kirstein et al., 2009).

This two-component Clp-protease system is highly conserved throughout prokaryotes and is also found in mitochondria and chloroplast of eukaryotes. Furthermore, it shares functional and architectural features with other energy-dependent protease systems such as HslVU in prokaryotes and the 26S proteasome in eukaryotes (Bochtler et al., 1999; Pickart and Cohen, 2004; Rohrwild et al., 1996; Song et al., 2000; Yu and Houry, 2007). Structural and biochemical studies of these ATP-dependent proteases have provided a wealth of information regarding the mechanism of substrate recognition and protease activation (Bochtler et al., 2000; Lee et al., 2010a; Park and Song, 2008; Park et al., 2007; Rabl et al., 2008; Ramachandran et al., 2002; Song et al., 2000; Sousa et al., 2000; Wang et al., 2001). HslU, ClpA/ClpX and the 19S regulatory cap utilize a domain(s) for recognizing substrate proteins and delivering these in an unfolded form, generated by ATP hydrolysis, to the matching proteases (Bochtler et al., 1999; Park and Song, 2008; Park et al., 2007; Sauer and Baker, 2011; Song and Eck, 2003). Structural studies of HslVU complex, ClpP in complex with activator acyldepsipeptide (ADEP), the 20S proteasome in complex with the 11S proteasome activator PA28, and the C-terminal peptide of proteasome-activating nucleosidase (PAN) have revealed the activation mechanism of the protease components (Lee et al., 2010a; Li et al., 2010; Rabl et al., 2008; Sousa et al., 2000; 2002; Stadtmueller and Hill, 2011; Whitby et al., 2000). As already mentioned, the cylindrical shape of the protease component has two substrate entry pores at both ends doubly capped by two AAA+ ATPases. All of these protease components are self-compartmentalized proteases that possess catalytic residues located deep inside the molecule, and which are shielded from direct access from the outside. It is unknown how the hydrolyzed products generated inside the protease chamber are efficiently released since all atomic resol-

School of Life Sciences and Biotechnology, Korea University, Seoul 136-701, Korea
*Correspondence: hksong@korea.ac.kr

Received September 17, 2011; revised October 11, 2011; accepted October 12, 2011; published online November 9, 2011

Keywords: *Bacillus*, ClpP, ClpXP, proteasome, side pore

ution structures of HslV, ClpP and the 20S proteasome show virtually no product exit site except for the entrance pores (Bochtler et al., 1999; Groll et al., 1997; Lowe et al., 1995; Song et al., 2000; 2003; Sousa et al., 2000; Wang et al., 1997; 2001; Yu and Houry, 2007).

Among the Clp-family of proteases, ClpP is the best characterized protease structurally, and possesses a unique region referred to as the 'handle region' utilized for upper and lower heptameric ring contacts. Presently, the structures of ClpPs from a variety of species have been reported (El Bakkouri et al., 2010; Kang et al., 2004; Kim and Kim, 2008; Lee et al., 2010a; Wang et al., 1997; Yu and Houry, 2007). In contrast to the similar overall architectural shape, a ClpP structure from *Mycobacterium tuberculosis* suggests a flexible ring-ring contact (Ingvarsson et al., 2007). An elegant quantitative NMR study of *E. coli* ClpP (EcClpP) suggested the presence of dynamic pores for peptide release, although clear structural information on this pore remains to be determined (Sprangers et al., 2005). A very recent structural study using ClpP from *Staphylococcus aureus* (SaClpP) showed a compressed structure of the ClpP rings, and identified side pores which are wide enough for product release (Geiger et al., 2011; Zhang et al., 2011). Subsequent biochemical assays have confirmed that this compressed structure of ClpP represents the state for product release.

Here, we present the structures of ClpP from *Bacillus subtilis* (BsClpP) in the compressed state as well as in the inhibited state with diisopropylfluoro-phosphate (DFP), a covalent serine protease inhibitor. The current study contributes structural information pertaining to several different conformational steps such as those related to extended, ADEP-activated, DFP-inhibited and compressed forms of ClpP from *B. subtilis*. The compressed structure of BsClpP shows an unusual structural feature in the handle region for regulating substrate exit, and this finding might provide the framework for understanding the general functional cycle of cylindrical proteases.

MATERIALS AND METHODS

Sample preparation

BsClpP was prepared as previously reported (Lee et al., 2010a). Briefly, BsClpP was cloned into pET-26b vector containing a six-residue histidine affinity tag at the carboxyl-terminus and then transformed into BL21(DE3). Expression was induced at 37°C by the addition of 1 mM IPTG at 0.7 OD (600 nm). Disrupted cell lysate was purified using His-trap Ni-NTA column, Hi-trap Q column and Superose 6 GL gel filtration chromatography (GE-healthcare). Purified BsClpP protein was concentrated to 4-5 mg/ml in buffer containing Tris-HCl (pH 8.0), 100 mM NaCl, 5% (w/v) glycerol and 1 mM DTT. For the preparation of DFP-inhibited enzyme, BsClpP and DFP were mixed in a 1:30 molar ratio and incubated for at least 30 min at 4°C.

Crystallization and data collection

All crystallizations were performed using the hanging-drop vapor-diffusion method at 22°C. Crystals of compressed-BsClpP were obtained using reservoir conditions comprising 100 mM sodium citrate (pH 5.6), 100 mM Li_2SO_4 and 10-12% (w/v) PEG 4000. The same crystallization produced two different crystal forms, compressed BsClpP with space group C2 (Table 1) and extended BsClpP with space group $P2_12_12$ (PDB ID: 3KTH) (Lee et al., 2010a). For the cryo-experiment, a single crystal was transferred to the reservoir solution containing 20% (w/v) glycerol prior to flash-freezing in a nitrogen stream at -173°C. DFP-inhibited BsClpP crystals were obtained using a reservoir solution comprising 100 mM Bicine/Trizma base (pH 8.5), 30 mM magnesium chloride, 30 mM calcium chloride, 20% (v/v) glycerol and 10% (w/v) PEG 4000 (Gorrec, 2009). Diffraction data were processed with the program HKL2000 (Otwinowski and Minor, 1997). Data collection statistics are summarized in Table 1.

Structure determination and refinement

Structures were determined by the molecular replacement method using the program MOLREP (Vagin and Teplyakov, 2010). The phases of compressed-BsClpP and DFP-inhibited BsClpP were obtained using ClpP from *Mycobacterium tuberculosis* (PDB ID: 2CE3) and the previously extended-BsClpP structure (PDB ID: 3KTG) as search models, respectively (Ingvarsson et al., 2007; Lee et al., 2010a). The model was rebuilt using the program COOT (Emsley et al., 2010). The position of DFP was clearly identified using a F_O-F_C difference Fourier map contoured at 2.5σ. Structures were refined using the program PHENIX (Adams et al., 2010). Final refinement statistics are also summarized in Table 1. For the structural comparisons, we used the coordinates of compressed ClpP from *Staphylococcus aureus* (PDB ID: 3QWD) (Geiger et al., 2011).

Accession codes

Protein Data Bank: Atomic coordinates and structure factors have been deposited with the following accession codes: 3TT6 for compressed BsClpP and 3TT7 for DFP-inhibited BsClpP.

RESULTS AND DISCUSSION

Structure of BsClpP in the compressed state

We obtained a crystal of BsClpP belonging to monoclinic space group C2 possessing different cell parameters to that of a previously determined structure (Table 1) (Lee et al., 2010a). Using the previous BsClpP model (PDB ID: 3KTG), we unsuccessfully attempted to solve the phase problem by molecular replacement. However, using a more distantly related starting model, a structure of ClpP1 from *M. tuberculosis* (MtClpP1, PDB ID: 2CE3), which possesses an unusual ClpP structure (Ingvarsson et al., 2007), gave a successful solution. Following extensive model rebuilding and refinement, we obtained the final model refined at 2.6 Å resolution with disordered residues at the axial loop and handle region in each monomer (residues 1-18 and 125-137), as in the case of MtClpP1 (Ingvarsson et al., 2007).

The overall structure of this new crystal form of BsClpP shows a root-mean-square (RMS) deviation of approximately 0.95 Å for 158 matching Cα atoms, suggesting a high degree of structural similarity to that of MtClpP1. This structure differs markedly from the previously determined BsClpP structure, even in overall shape, and shows that it is axially compressed by ca. 15 Å and slightly equatorially expanded by ca. 2 Å (Fig. 1). Here, this structure is referred to as a compressed form of ClpP, whereas the previously determined BsClpP structure is referred to as an extended form. When the compressed BsClpP structure was analyzed, the presence of 14 pores generated by disordered residues at handle regions in the equatorial side was immediately apparent (Fig. 1B). It is intriguing that the exit site for proteolytic products in ClpP remains unclear since all reported structures of ClpP only have two axial pores for substrate entry, which are capped by two Clp-ATPases (Fig. 1B) (Lee et al., 2010a; 2010b; Yu and Houry, 2007). Structural studies have suggested possibilities such as a singly capped ClpXP/ClpAP complex, which permits product release by one of two axial pores, and labile doubly-capped species, in which

Table 1. Crystallographic data

	Compressed	DFP-inhibited
Data Collection		
Space Group	C2	C2
a, b, c	109.09, 172.87, 83.43	122.34, 152.0, 110.07
α, β, γ	90, 118.93, 90	90, 113.21, 90
Wavelength (Å)	1.0000	0.9000
Resolution (Å)	2.60 (2.60-2.69)	2.55 (2.55-2.59)
R_{sym} (%)	5.8 (34.7)	5.4 (31.5)
$I / I (\sigma)$	30.0 (2.4)	26.2 (3.4)
Total reflections	136,757	156,052
Unique reflections	41,517	52,506
Completeness (%)	94.6 (99.4)	88.3 (83.0)
Redundancy	3.6 (3.3)	2.3 (3.0)
Refinement		
Resolution range (Å)	36.09-2.60	37.12-2.55
Reflections used	41,349	51,513
R_{work} / R_{free} (%)	22.4 / 25.9	21.7 / 28.0
Number of atoms		
Protein	8,574	9,576
Ligand	-	70 (DFP)
Water	28	176
B-factors (Å)		
Protein	70.0	42.6
Ligand	-	53.3 (DFP)
Water	62.7	40.9
RMS deviations		
Bond length (Å)	0.013	0.010
Bond angle (°)	1.354	1.333
Ramachandran plot (%)		
Most favored	94.5	97.3
Additional allowed	4.4	2.1
Generously allowed	1.1	0.2
Disallowed	0.0	0.5

Clp-ATPase continuously dissociates and re-associates with ClpP (Ortega et al., 2002; 2004). However, it has been reported that the handle regions utilized in ring-to-ring contacts in ClpP are highly dynamic and potential product exit sites as determined by NMR experiments in combination with biochemical studies and later in structural and theoretical studies using mutant enzymes (Kimber et al., 2010; Sprangers et al., 2005). Therefore, the side pores found in our compressed BsClpP must represent product exit sites for the efficient enzymatic cycle (Fig. 1B). While analyzing our compressed BsClpP structure, a similar compressed ClpP structure from *S. aureus* was reported (Fig. 1C) (Geiger et al., 2011; Zhang et al., 2011). Although it also shows a significantly compressed structure, the details differ substantially (See details later).

Differences between compressed and extended forms

Although there are marked overall structural differences between the extended and compressed forms of BsClpP (Figs. 1A and 1B), the secondary and tertiary structures of both forms of ClpP are very similar except for the dynamic handle region (Fig. 2A). As shown in Fig. 2B, a portion of the loop between α5 and β6 in handle region forms a β-sheet with that handle region opposite the heptameric ring, whereas a portion of the loop and helix α5 (residues 125-137) in compressed BsClpP are disordered in electron density, suggesting high flexibility of this region. Subsequently, there is no β-sheet formation between handle regions of the monomers in the two opposite heptameric rings (Figs. 1 and 2B). Given this disorder, the equatorial side of ClpP possesses larger pores which are wide enough to release proteolytic product (Fig. 1B). Indeed, the mutation of Glu135 and Leu144 in the handle region of SaClpP to opposite charged or alanine residues abolishes the catalytic activity due to a defect of product release (Geiger et al., 2011). The existence of side exit pores is essential for achieving the optimal proteolytic efficiency of 2:1 ClpXP or ClpAP complexes because both ends of ClpP cylinder are capped by Clp-ATPases (Maglica et al.,

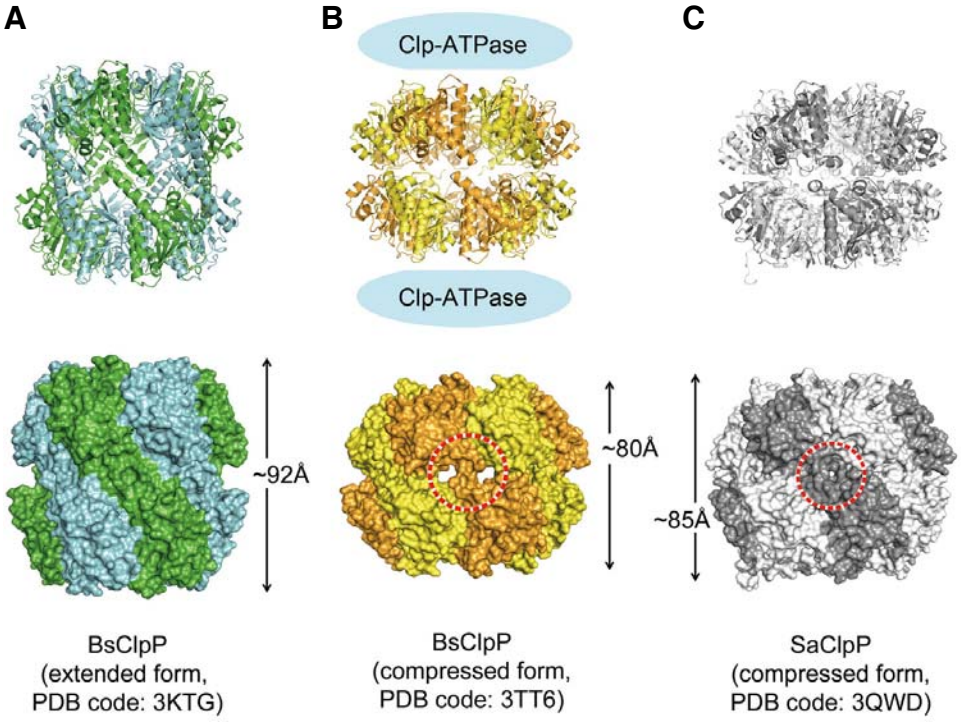

Fig. 1. Overall structure of ClpPs from *B. subtilis* and *S. aureus*. (A) Structure of ClpP from *B. subtilis* in the extended state shown as a ribbon diagram (top) and surface representation (bottom) viewed along a two-fold symmetry axis. Monomers are alternately colored green and sky-blue. (B) Structure of ClpP from *B. subtilis* in the compressed state with the same view and representation as in (A). Monomers are alternately colored yellow and orange. The location of two Clp-ATPases is shown as sky-blue ovals. (C) Structure of ClpP from *S. aureus* in the compressed state with the same view and representation as in (A). Monomers are alternately colored dark and bright gray. PDB IDs are provided. The approximate height of the molecules in this side view is indicated and the side pore utilized for product release is also shown as a red dotted circle.

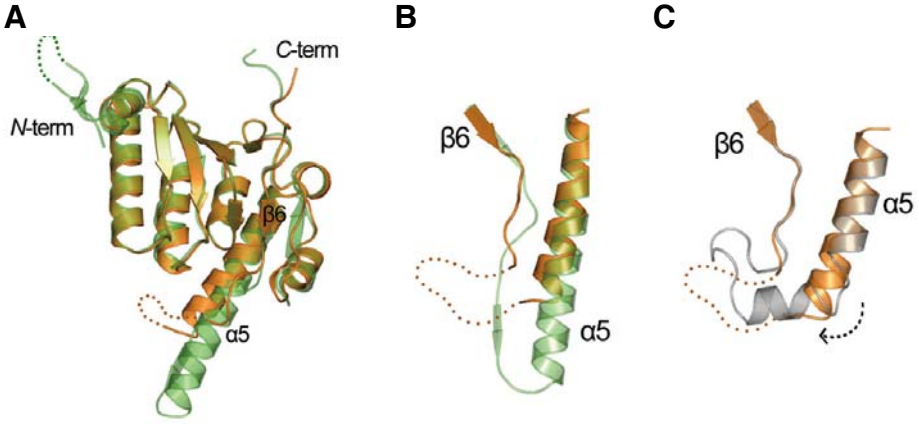

Fig. 2. Superposition of compressed and extended ClpP structures. (A) Compressed (orange) and extended (green) BsClpP monomer. The N- and C-terminus are labeled. Large conformational differences are found in the handle region, especially within α5-helix and β6-strand regions. (B) Close-up view of the region representing the greatest difference between compressed (orange) and extended (green) BsClpP. (C) Close-up view of the region representing the greatest difference between compressed BsClpP (orange) and SaClpP (slate). Invisible portions of the structures are shown as dots in all panels.

2009).

The active site was then analyzed since the catalytic triad (Ser97-His122-Asp171) in ClpP is located in the cleft between the head domain and handle region (Wang et al., 1997). Previously, we reported that the catalytic triads in extended and ADEP-bound activated BsClpP showed very similar conformations, ruling out an allosteric activation mechanism (Lee et al., 2010a). Interestingly, the distance between Ser97 and His112 in the compressed form increased by approximately up to 7 Å due to the different orientation of the side chain imidazole ring of His122 (Fig. 3A), and consequently the active sites are severely distorted and must be enzymatically inactive compared to the 2.8 Å distance present in catalytically competent serine proteases (Fig. 3A) (Kim and Kim, 2008; Lee et al., 2010a; Park et al., 2004). In fact, this histidine movement might be caused by an approximate 2 Å shift of the main chain segment containing Asp171 (Fig. 3A).

Comparison of compressed ClpPs from two different species

As we noted, a similar compressed structure of ClpP from *S. aureus* has been reported independently (Geiger et al., 2011). Although both structures are compressed along the axial pore, BsClpP is further compressed by approximately 5 Å compared to SaClpP (Fig. 1C). As a consequence, BsClpP possesses larger side pores compared with SaClpP. This difference can be accounted for by considering the handle region in SaClpP which, as in the case of BsClpP, shows a different conformation from the extended ClpP structures, although the detailed conformations of BsClpP and SaClpP differ markedly (Fig. 2C).

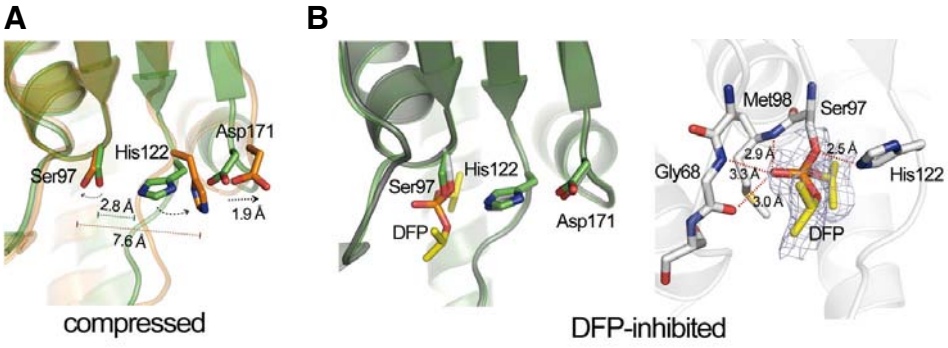

Fig. 3. Active site of ClpPs. (A) Comparison of catalytic triad of compressed (orange) and extended (green) BsClpP. Ser97, His122 and Asp171 are shown as stick models with nitrogen and oxygen atoms in blue and red, respectively. The H-bonding distances between side chain atoms of Ser97 and His122 in two different structural states are indicated. (B) Structure of DFP-inhibited BsClpP superposed with that of extended BsClpP (left) and its corresponding electron density for the DFP-inhibited covalently modified molecule (right). H-bonding distances are indicated.

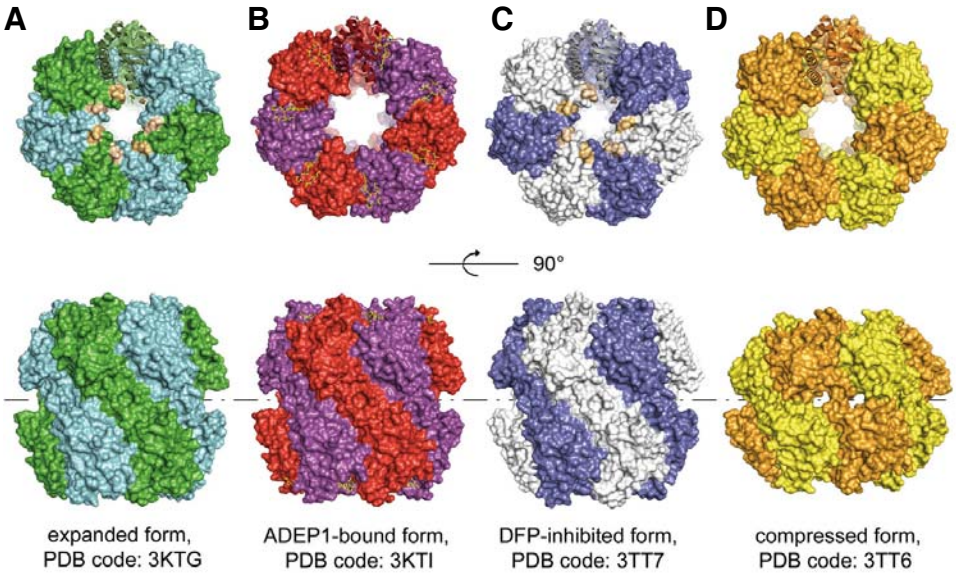

Fig. 4. Structural comparison of 4 different states of ClpP. (A) Molecular surface representation of the extended BsClpP structure viewed along a sevenfold molecular symmetry axis (top) and 90° rotation to display the side two-fold symmetry axis (bottom). The colors are the same as in Fig. 1A and one monomer is shown as a dark green ribbon for clarity. (B) The same representation as with ADEP1-bound BsClpP. Monomers are alternately colored red and purple, with one monomer shown as a dark red ribbon and bound ADEP1 molecules are shown as stick models with carbon, nitrogen and oxygen atoms in yellow, blue and red, respectively. (C) The same representation as with DFP-inhibited BsClpP. Monomers are alternately colored white and slate, with one monomer shown as a grey ribbon. (D) The same representation as with the compressed BsClpP structure. The colors are the same as in Fig. 1B and one monomer is shown in dark orange. The N-terminal β-1 strand is colored apricot for clarity in (A) and (C). PDB IDs are provided for each different structural state.

Two-thirds of the characteristic long helix α5 in the handle region is melted down and invisible in BsClpP, suggesting multiple conformations due to its extreme flexibility, whereas the helix in SaClpP is kinked sharply and whole residues in this region are well-defined (Fig. 2C). Although there is a difference in the local conformation, the consequence of this structural change in helix α5 opens the side exit pores for product release. It has been reported that the catalytic triad of SaClpP is also catalytically inactive and basically adopts a similar conformation to that found in our compressed BsClpP (Fig. 3A) (Geiger et al., 2011).

Structure of DFP-Inhibited BsClpP

In an effort to determine whether the overall conformational changes are induced by inhibition of the active site of BsClpP, we also determined the crystal structure of BsClpP inhibited by diisopropylfluoro-phosphate (DFP), a well-known serine protease inhibitor that covalently binds to serine residues at the catalytic dyad and triad of proteases. The structure of the BsClpP-DFP complex was determined at 2.55 Å resolution (Table 1) and the catalytic serine residue (Ser97) of all active sites was found to be covalently modified with DFP (Fig. 3B). The overall structure of the BsClpP-DFP complex is essentially the same as that of free (extended) BsClpP (RMS deviation of 0.37 Å for 180 matching Cα atoms in each monomer), confirming no major conformational change of ClpP upon DFP-inhibition. Even superposition of catalytic triads of extended and DFP-inhibited BsClpP shows nearly identical orientation of side chain atoms (Fig. 3B).

Conformational diversity of ClpP

This BsClpP as well as ScClpP showed a compressed structure containing pores on the equatorial side of the cylindrical barrel, and confirms the substrate releasing exit route proposed by previous biochemical and mutational studies (Kimber et al., 2010; Sprangers et al., 2005), although the details differ depending on the bacterial species as described above. We further analyzed the other functionally important regions in ClpP.

The N-terminal segments (residues 1-18) near the axial pore region could not be built in our compressed BsClpP structure

(Fig. 4D), although portions of segments including residues of strand β-1 in extended BsClpP were well-defined (Fig. 4A) (Lee et al., 2010a). These different features of the axial pore region are also found in MtClpP1, in which 15 residues at the amino-terminus of MtClpP1 are also disordered (Ingvarsson et al., 2007). Furthermore, the same N-terminal segments in ADEP-bound BsClpP were completely disordered, whereas those in ADEP-bound EcClpP were ordered (Lee et al., 2010a; Li et al., 2010). In contrast to compressed BsClpP, compressed SaClpP has well-defined N-terminal segments as well as handle regions (Geiger et al., 2011). In addition to the axial pore, we investigated the active site of ClpP. Previously, several ClpP structures representing inhibited or substrate-bound states have been reported (Kim and Kim, 2008; Szyk and Maurizi, 2006; Wang et al., 1997). The overall shape of all of these structures shows an extended conformation as in the case of DFP-inhibited BsClpP, although the active sites and N-terminal segments of the apo and inhibited structures vary depending on the bacterial species. For example, apo ClpP from *H. pyroli* (HpClpP) and EcClpP possess an inactive catalytic triad and undergo structural rearrangement upon substrate or inhibitor binding (Kim and Kim, 2008; Szyk and Maurizi, 2006), whereas BsClpP shows a structurally competent catalytic triad even in the apo state (Lee et al., 2010a). As noted above, the catalytic triad in compressed structures from the same species shows a severely distorted conformation (Fig. 3A). With respect to the N-terminal segments, apo HpClpP possesses a disordered conformation as in the case of ADEP-bound BsClpP (Fig. 4B), showing an enlarged axial pore without activator (Kim and Kim, 2008). Indeed, the conformation of the N-terminal segments remains unclear since several different structures have been reported such as disordered, asymmetric up-and-down, and ordered with activator or inhibitor, even in the same species (*E. coli*) (Bewley et al., 2006; Li et al., 2010; Szyk and Maurizi, 2006; Wang et al., 1997). In our DFP-inhibited structure, the N-terminal segments are well ordered and form a relatively narrow axial pore (Fig. 4C), however the pore is enlarged in the compressed structure (Fig. 4D). Hence, it is tempting to speculate that this flexible region possesses a dynamic property depending on the functional status, and may play a critical role in communicating with protein activator Clp-ATPases.

In conclusion, it should be noted that many of the functionally important regions in ClpP-family proteases such as N-terminal segments for the axial pore, catalytic triads, and handle domains associated with the product releasing pore exhibit intrinsically dynamic and unique structural features which are present within and between species. Therefore, it is important to acquire structural information pertaining to a series of structural states from the same species as shown in Fig. 4. The BsClpP structures representing 4 different states should prove useful in contributing towards an understanding of this enigmatic cylindrical degradation machinery, and might form the basis for delineating the mechanisms utilized by other proteases such as HslV and the 20S proteasome.

ACKNOWLEDGMENTS

We thank the staff at 4A beamline, Pohang Accelerator Laboratory, Korea, and BL44XU beamline, Spring-8, Japan for help with the data collection. This work was supported by the Korea Healthcare Technology R&D Project (A084016), Ministry for Health, Welfare and Family Affairs.

REFERENCES

Adams, P.D., Afonine, P.V., Bunkoczi, G., Chen, V.B., Davis, I.W., Echols, N., Headd, J.J., Hung, L.W., Kapral, G.J., Grosse-Kunstleve, R.W., et al. (2010). PHENIX: a comprehensive Python-based system for macromolecular structure solution. Acta Crystallogr. D Biol. Crystallogr. *66*, 213-221.

Baker, T.A., and Sauer, R.T. (2006). ATP-dependent proteases of bacteria: recognition logic and operating principles. Trends Biochem. Sci. *31*, 647-653.

Bewley, M.C., Graziano, V., Griffin, K., and Flanagan, J.M. (2006). The asymmetry in the mature amino-terminus of ClpP facilitates a local symmetry match in ClpAP and ClpXP complexes. J. Struct. Biol. *153*, 113-128.

Bochtler, M., Ditzel, L., Groll, M., Hartmann, C., and Huber, R. (1999). The proteasome. Annu. Rev. Biophys. Biomol. Struct. *28*, 295-317.

Bochtler, M., Hartmann, C., Song, H.K., Bourenkov, G.P., Bartunik, H.D., and Huber, R. (2000). The structures of HslU and the ATP-dependent protease HslU-HslV. Nature *403*, 800-805.

El Bakkouri, M., Pow, A., Mulichak, A., Cheung, K.L., Artz, J.D., Amani, M., Fell, S., de Koning-Ward, T.F., Goodman, C.D., McFadden, G.I., et al. (2010). The Clp chaperones and proteases of the human malaria parasite *Plasmodium falciparum*. J. Mol. Biol. *404*, 456-477.

Emsley, P., Lohkamp, B., Scott, W.G., and Cowtan, K. (2010). Features and development of Coot. Acta Crystallogr. D Biol. Crystallogr. *66*, 486-501.

Geiger, S.R., Bottcher, T., Sieber, S.A., and Cramer, P. (2011). A conformational switch underlies ClpP protease function. Angew. Chem. Int. Ed. Engl. *50*, 5749-5752.

Gorrec, F. (2009). The MORPHEUS protein crystallization screen. J. Applied Crystallogr. *42*, 1035-1042.

Gottesman, S. (2003). Proteolysis in bacterial regulatory circuits. Annu. Rev. Cell Dev. Biol. *19*, 565-587.

Groll, M., Ditzel, L., Lowe, J., Stock, D., Bochtler, M., Bartunik, H.D., and Huber, R. (1997). Structure of 20S proteasome from yeast at 2.4 A resolution. Nature *386*, 463-471.

Ingvarsson, H., Mate, M.J., Hogbom, M., Portnoi, D., Benaroudj, N., Alzari, P.M., Ortiz-Lombardia, M., and Unge, T. (2007). Insights into the inter-ring plasticity of caseinolytic proteases from the X-ray structure of Mycobacterium tuberculosis ClpP1. Acta Crystallogr. D Biol. Crystallogr. *63*, 249-259.

Kang, S.G., Maurizi, M.R., Thompson, M., Mueser, T., and Ahvazi, B. (2004). Crystallography and mutagenesis point to an essential role for the N-terminus of human mitochondrial ClpP. J. Struct Biol. *148*, 338-352.

Kim, D.Y., and Kim, K.K. (2008). The structural basis for the activation and peptide recognition of bacterial ClpP. J. Mol. Biol. *379*, 760-771.

Kimber, M.S., Yu, A.Y., Borg, M., Leung, E., Chan, H.S., and Houry, W.A. (2010). Structural and theoretical studies indicate that the cylindrical protease ClpP samples extended and compact conformations. Structure *18*, 798-808.

Kirstein, J., Moliere, N., Dougan, D.A., and Turgay, K. (2009). Adapting the machine: adaptor proteins for Hsp100/Clp and AAA+ proteases. Nat. Rev. Microbiol. *7*, 589-599.

Lee, B.G., Park, E.Y., Lee, K.E., Jeon, H., Sung, K.H., Paulsen, H., Rubsamen-Schaeff, H., Brotz-Oesterhelt, H., and Song, H.K. (2010a). Structures of ClpP in complex with acyldepsipeptide antibiotics reveal its activation mechanism. Nat. Struct. Mol. Biol. *17*, 471-478.

Lee, M.E., Baker, T.A., and Sauer, R.T. (2010b). Control of substrate gating and translocation into ClpP by channel residues and ClpX binding. J. Mol. Biol. *399*, 707-718.

Li, D.H., Chung, Y.S., Gloyd, M., Joseph, E., Ghirlando, R., Wright, G.D., Cheng, Y.Q., Maurizi, M.R., Guarne, A., and Ortega, J. (2010). Acyldepsipeptide antibiotics induce the formation of a structured axial channel in ClpP: a model for the ClpX/ClpA-bound state of ClpP. Chem. Biol. *17*, 959-969.

Lowe, J., Stock, D., Jap, B., Zwickl, P., Baumeister, W., and Huber, R. (1995). Crystal structure of the 20S proteasome from the archaeon T. acidophilum at 3.4 A resolution. Science *268*, 533-539.

Maglica, Z., Kolygo, K., and Weber-Ban, E. (2009). Optimal efficiency of ClpAP and ClpXP chaperone-proteases is achieved by architectural symmetry. Structure *17*, 508-516.

Ortega, J., Lee, H.S., Maurizi, M.R., and Steven, A.C. (2002). Alternating translocation of protein substrates from both ends of ClpXP protease. EMBO J. *21*, 4938-4949.

Ortega, J., Lee, H.S., Maurizi, M.R., and Steven, A.C. (2004). ClpA and ClpX ATPases bind simultaneously to opposite ends of ClpP peptidase to form active hybrid complexes. J. Struct. Biol. *146*, 217-226.

Otwinowski, Z., and Minor, W. (1997). Processing of X-ray diffraction data collected in oscillation mode. Method Enzymol. *276*, 307-326.

Park, E.Y., and Song, H.K. (2008). A degradation signal recognition in prokaryotes. J. Synchrotron Radiat. *15*, 246-249.

Park, E.Y., Kim, J.A., Kim, H.W., Kim, Y.S., and Song, H.K. (2004). Crystal structure of the Bowman-Birk inhibitor from barley seeds in ternary complex with porcine trypsin. J. Mol. Biol. *343*, 173-186.

Park, E.Y., Lee, B.G., Hong, S.B., Kim, H.W., Jeon, H., and Song, H.K. (2007). Structural basis of SspB-tail recognition by the zinc binding domain of ClpX. J. Mol. Biol. *367*, 514-526.

Pickart, C.M., and Cohen, R.E. (2004). Proteasomes and their kin: proteases in the machine age. Nat. Rev. Mol. Cell Biol. *5*, 177-187.

Rabl, J., Smith, D.M., Yu, Y., Chang, S.C., Goldberg, A.L., and Cheng, Y. (2008). Mechanism of gate opening in the 20S proteasome by the proteasomal ATPases. Mol. Cell *30*, 360-368.

Ramachandran, R., Hartmann, C., Song, H.K., Huber, R., and Bochtler, M. (2002). Functional interactions of HslV (ClpQ) with the ATPase HslU (ClpY). Proc. Natl. Acad. Sci. USA *99*, 7396-7401.

Rohrwild, M., Coux, O., Huang, H.C., Moerschell, R.P., Yoo, S.J., Seol, J.H., Chung, C.H., and Goldberg, A.L. (1996). HslV-HslU: A novel ATP-dependent protease complex in *Escherichia coli* related to the eukaryotic proteasome. Proc. Natl. Acad. Sci. USA *93*, 5808-5813.

Sauer, R.T., and Baker, T.A. (2011). AAA+ Proteases: ATP-fueled machines of protein destruction. Annu. Rev. Biochem. *80*, 587-612.

Song, H.K., and Eck, M.J. (2003). Structural basis of degradation signal recognition by SspB, a specificity-enhancing factor for the ClpXP proteolytic machine. Mol. Cell *12*, 75-86.

Song, H.K., Hartmann, C., Ramachandran, R., Bochtler, M., Behrendt, R., Moroder, L., and Huber, R. (2000). Mutational studies on HslU and its docking mode with HslV. Proc. Natl. Acad. Sci. USA *97*, 14103-14108.

Song, H.K., Bochtler, M., Azim, M.K., Hartmann, C., Huber, R., and Ramachandran, R. (2003). Isolation and characterization of the prokaryotic proteasome homolog HslVU (ClpQY) from Thermotoga maritima and the crystal structure of HslV. Biophys. Chem. *100*, 437-452.

Sousa, M.C., Trame, C.B., Tsuruta, H., Wilbanks, S.M., Reddy, V.S., and McKay, D.B. (2000). Crystal and solution structures of an HslUV protease-chaperone complex. Cell *103*, 633-643.

Sousa, M.C., Kessler, B.M., Overkleeft, H.S., and McKay, D.B. (2002). Crystal structure of HslUV complexed with a vinyl sulfone inhibitor: corroboration of a proposed mechanism of allosteric activation of HslV by HslU. J. Mol. Biol. *318*, 779-785.

Sprangers, R., Gribun, A., Hwang, P.M., Houry, W.A., and Kay, L.E. (2005). Quantitative NMR spectroscopy of supramolecular complexes: dynamic side pores in ClpP are important for product release. Proc. Natl. Acad. Sci. USA *102*, 16678-16683.

Stadtmueller, B.M., and Hill, C.P. (2011). Proteasome activators. Mol. Cell *41*, 8-19.

Szyk, A., and Maurizi, M.R. (2006). Crystal structure at 1.9A of E. coli ClpP with a peptide covalently bound at the active site. J. Struct. Biol. *156*, 165-174.

Vagin, A., and Teplyakov, A. (2010). Molecular replacement with MOLREP. Acta Crystallogr. D Biol. Crystallogr. *66*, 22-25.

Wang, J., Hartling, J.A., and Flanagan, J.M. (1997). The structure of ClpP at 2.3 A resolution suggests a model for ATP-dependent proteolysis. Cell *91*, 447-456.

Wang, J., Song, J.J., Franklin, M.C., Kamtekar, S., Im, Y.J., Rho, S.H., Seong, I.S., Lee, C.S., Chung, C.H., and Eom, S.H. (2001). Crystal structures of the HslVU peptidase-ATPase complex reveal an ATP-dependent proteolysis mechanism. Structure *9*, 177-184.

Whitby, F.G., Masters, E.I., Kramer, L., Knowlton, J.R., Yao, Y., Wang, C.C., and Hill, C.P. (2000). Structural basis for the activation of 20S proteasomes by 11S regulators. Nature *408*, 115-120.

Yu, A.Y., and Houry, W.A. (2007). ClpP: a distinctive family of cylindrical energy-dependent serine proteases. FEBS Lett. *581*, 3749-3757.

Zhang, J., Ye, F., Lan, L., Jiang, H., Luo, C., and Yang, C.G. (2011). Structural switching of Staphylococcus aureus ClpP: a key to understanding protease dynamics. J. Biol. Chem. *286*, 37590-37601.